ORIGINAL PAPER



Nonprehensile manipulation of a stick using impulsive forces

Aakash Khandelwal · Nilay Kant · Ranjan Mukherjee ·

Received: 28 June 2022 / Accepted: 13 August 2022 © The Author(s), under exclusive licence to Springer Nature B.V. 2022

Abstract The problem of nonprehensile manipulation of a stick in three-dimensional space using intermittent impulsive forces is considered. The objective is to juggle the stick between a sequence of configurations that are rotationally symmetric about the vertical axis. The dynamics of the stick is described by five generalized coordinates and three control inputs. Between two consecutive configurations where impulsive inputs are applied, the dynamics is conveniently represented by a Poincaré map in the reference frame of the juggler. Stabilization of the orbit associated with a desired juggling motion is accomplished by stabilizing a fixed point on the Poincaré map. The Impulse Controlled Poincaré Map approach is used to stabilize the orbit, and numerical simulations are used to demonstrate convergence to the desired juggling motion from an arbitrary initial configuration. In the limiting case, where consecutive rotationally symmetric configurations are chosen arbi-

Supplementary Information The online version contains supplementary material available at https://doi.org/10.1007/s11071-022-07826-4.

A. Khandelwal · N. Kant · R. Mukherjee (⊠) Department of Mechanical Engineering, Michigan State University, East Lansing, MI 48824, USA e-mail: mukherji@egr.msu.edu

A. Khandelwal

e-mail: khande10@egr.msu.edu

Published online: 26 September 2022

N. Kant

e-mail: kantnila@msu.edu

trarily close, it is shown that the dynamics reduces to that of steady precession of the stick on a hoop.

Keywords Nonprehensile manipulation · Juggling · Impulsive force · Poincaré map · Orbital stabilization

List of symbols

g	Acceleration due to gravity (m/s ²)
h_x, h_y, h_z	Cartesian coordinates of the center-of-
	mass of the stick in the xyz frame (m)
ℓ	Length of the stick (m)
m	Mass of the stick (kg)
r	Distance of point of application of impul-
	sive force from the center-of-mass of the
	stick, measured positive along the z_2 -axis
	(m)
v_x, v_y, v_z	Velocities of the center-of-mass of the
	stick in the xyz frame (m/s)
xyz	Inertial reference frame
$x_0 y_0 z_0$	Reference frame with origin at the center-
	of-mass of the stick; aligned with the xyz
	frame
$x_1 y_1 z_1$	Reference frame with origin at the center-
	of-mass of the stick; obtained by rotating
	$x_0y_0z_0$ frame by α about the z_0 -axis
$x_2y_2z_2$	Reference frame with origin at the center-
	of-mass of the stick; obtained by rotating
	$x_1y_1z_1$ frame by β about the y_1 -axis



$x_3 y_3 z_3$	Body-fixed reference frame with ori-
	gin at the center-of-mass of the stick;
	obtained by rotating $x_2y_2z_2$ frame by γ
	about the z_2 -axis
H_x , H_y , H_z	Components of the angular momentum
	about the center-of-mass of the stick in
	the xyz frame (kg m ² /s)
I	Nonnegative magnitude of impulsive
	force applied on the stick (Ns)
J	Mass moment of inertia of the stick about
	the principal axes x_3 and y_3 (kg m ²)
R	Rotation matrix that transforms a vec-
	tor from the $x_3y_3z_3$ frame to the $x_0y_0z_0$
	frame
α, β, γ	zyz Euler angle sequence describing the
	stick orientation (rad)
ϕ	Angle that the impulsive force makes
	with the x_2 -axis, measured positive about
	the z_2 -axis, lies in the interval $[-\pi/2,$
	$\pi/2$] (rad)
$\dot{lpha},\dot{eta},\dot{\gamma} \ ar{[.]}$	zyz Euler angle rates (rad/s)
ſ.j. , ,	[.] expressed in the reference frame of the
E-3	juggler
	3 00

1 Introduction

With robots expected to perform increasingly complex tasks, it is imperative that nonprehensile manipulation is included in their repertoire. Nonprehensile manipulation represents an important class of problems in which objects are manipulated without grasping; they are subjected to unilateral constraints and need not strictly follow the motion of the manipulator [12, 14–16,22,28]. The advantages of nonprehensile manipulation over prehensile manipulation [14,22] include:

- added flexibility in manipulation since additional surfaces of the manipulator may be used to make unilateral contact with the object.
- an increased workspace, exceeding the kinematic reach of the manipulator.
- the ability to control more degrees-of-freedom (DOFs) than that of the manipulator.

Nonprehensile manipulation can be subdivided into tasks where the contact between the manipulator and the object is continuous, and tasks where the contact is intermittent. Continuous contact occurs, for example, when an object is pushed by a manipulator to

slide or roll on a surface. Examples of the latter class of problems include the nonprehensile manipulation primitives of dynamic catching, throwing, and *batting* [22], which combines dynamic catching and throwing into a single collision. Juggling is a nonprehensile manipulation task comprised of iterative batting primitives [22]. The dynamics of juggling is hybrid (non-smooth) and involves the application of intermittent impulsive forces. The controllability and stability of hybrid dynamical systems has been investigated by many researchers [4–6,13,26,30], but is not the focus of this paper.

Juggling a point mass, such as a ball or a hockey puck, requires the application of a single impulsive force for each batting primitive to achieve a desired motion. The ball-juggling problem was investigated using a one-DOF table [29] first, and later using a two-DOF manipulator [3]. The work in [3] is, however, more extensive, and treats the feedback control of complementary-slackness juggling systems. Both [3,29] consider the complete dynamic model of the system, comprised of both the object and the robot, along with the associated unilateral constraint and impact rule. Blind-jugglers, which juggle balls without relying on external sensors, have been analyzed in [20,21], and other solutions to juggling of point masses have been proposed in [23,24,27]. Compared to a point mass, which is described by position coordinates only, a stick represents an extended object that is described by both position and orientation coordinates. Therefore, both the physical task and the mathematical problem of stick-juggling are more challenging than juggling a ball or a point mass.

Previous work on nonprehensile manipulation of sticks has documented the use of continuous-time inputs for rotary *propeller* motion [17, 18, 25] but there is limited literature on manipulation of sticks using impulsive forces. For nonprehensile manipulation of a stick using impulsive forces, the location, direction, and magnitude of the impulsive force have to be taken into consideration for every batting primitive. An openloop strategy for planar stick-juggling was presented by Schaal and Atkeson [24]; the dynamics of the system was, however, not completely modeled. The complete dynamic model and closed-loop control designs for planar stick-juggling were presented by Kant and Mukherjee in [9,10]. Nonprehensile manipulation of a stick in three-dimensional space has not appeared in the literature and this work is the first to present a hybrid



dynamic model that lends itself to closed-loop control design. The dynamic model represents an underactuated system with five generalized coordinates and three control inputs; the three-dimensional juggling problem is more challenging than the planar case where the stick is described by three generalized coordinates and two control inputs. The Impulse Controlled Poincaré Map (ICPM) approach [8,10], in which impulsive forces are intermittently applied on a Poincaré section, is used for stabilizing the hybrid orbit that describes the desired juggling motion.

This paper is organized as follows. The problem of juggling a stick in three-dimensional space using impulsive forces is formally stated in Sect. 2. The impulsive and continuous-time dynamics of the stick is presented in Sect. 3. The hybrid dynamics of the stick between two consecutive configurations where impulsive inputs are applied is described with the help of a nonlinear discrete-time Poincaré map in Sect. 4. The control design is presented in Sect. 5. Simulation results are presented in Sect. 6. Section 7 considers the special cases of planar juggling and steady precession. It is shown that previously derived expressions for planar symmetric juggling [9,10] can be recovered from the current, more general, formulation. The steady precession of the stick is shown to be a limiting case of the hybrid dynamics. Concluding remarks are provided in Sect. 8.

2 Problem description

Consider the six DOF stick shown in Fig. 1, which can move freely in three-dimensional space. The center-ofmass of the stick is denoted by G. The configuration of the stick is specified by the generalized coordinates $(h_x, h_y, h_z, \alpha, \beta, \gamma)$. The stick is assumed to be symmetric about the body-fixed z_3 -axis, which is the same as the z_2 -axis. Due to this axisymmetry, the rotation by γ about the z_2 -axis is imperceptible. The objective is to juggle the stick between a sequence of configurations which, at steady-state, are rotationally symmetric about the inertial z-axis—see Fig. 2. Each configuration in the sequence satisfies $\beta = \beta^*, \beta^* \in (0, \pi/2)$, and can be obtained from the previous configuration by a fixed change in α , equal to $\Delta \alpha^*$. For the sequence of configurations, the coordinates of G lie on a circle parallel to the xy plane. The stick is juggled using purely impulsive forces applied normal to the stick;

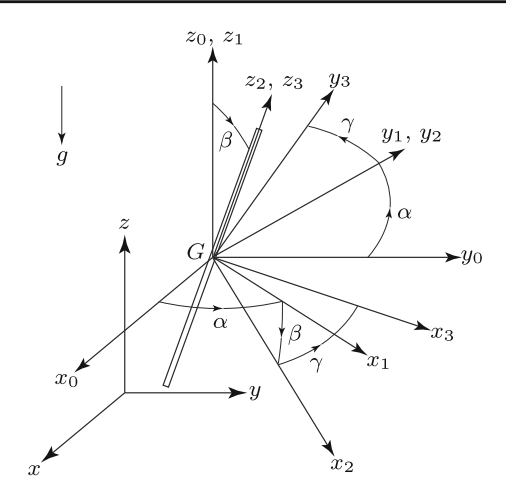


Fig. 1 A rigid stick in the three-dimensional space has six DOFs and is described by the configuration variables $(h_x, h_y, h_z, \alpha, \beta, \gamma)$

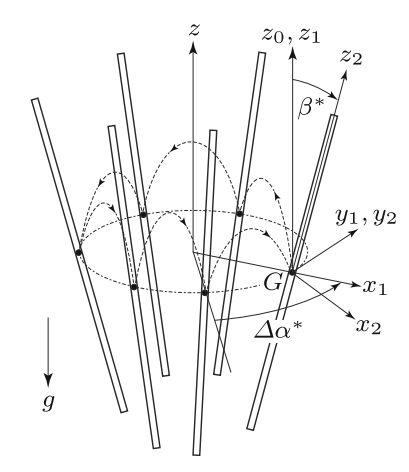


Fig. 2 A sequence of configurations of the stick at steady-state, rotationally symmetric about the *z*-axis

the impulsive forces are applied only when $\beta = \beta^*$. Since the impulsive force is applied normal to the stick, the impulsive force lies on a plane parallel to the x_2y_2 plane—see Fig. 3. The control inputs are the triplet (I, r, ϕ) ; at steady-state, they assume the constant values (I^*, r^*, ϕ^*) .

3 System dynamics

3.1 Coordinate transformations

The elementary rotation matrices describing a rotation about the *y*- and *z*-axes by angle θ are given as:



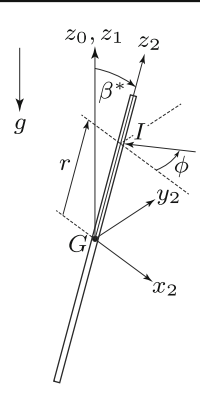


Fig. 3 Control inputs (I, r, ϕ) : the impulsive force is applied when $\beta = \beta^*$

$$\mathbf{R}_{y}(\theta) = \begin{bmatrix} \cos \theta & 0 \sin \theta \\ 0 & 1 & 0 \\ -\sin \theta & 0 \cos \theta \end{bmatrix}, \ \mathbf{R}_{z}(\theta) = \begin{bmatrix} \cos \theta & -\sin \theta & 0 \\ \sin \theta & \cos \theta & 0 \\ 0 & 0 & 1 \end{bmatrix}$$
(1)

A vector **p** described in the inertial reference frame can be related to the same vector expressed in the bodyfixed frame by the expression

$$\mathbf{p} = \mathbf{R}\mathbf{p}_{b}, \quad \mathbf{R} \stackrel{\triangle}{=} \mathbf{R}_{z}(\alpha)\mathbf{R}_{v}(\beta)\mathbf{R}_{z}(\gamma)$$
 (2)

We define the position and velocity vectors in the inertial frame

$$\mathbf{h} \triangleq \begin{bmatrix} h_x \\ h_y \\ h_z \end{bmatrix}, \quad \mathbf{v} \triangleq \begin{bmatrix} v_x \\ v_y \\ v_z \end{bmatrix} = \begin{bmatrix} \dot{h}_x \\ \dot{h}_y \\ \dot{h}_z \end{bmatrix}$$
(3)

The vector of Euler angle rates can be related to the angular velocity vector in the inertial frame using the relationship

$$\boldsymbol{\omega} = \mathbf{S}\boldsymbol{\Omega}, \ \mathbf{S} \triangleq \begin{bmatrix} 0 - \sin\alpha \cos\alpha \sin\beta \\ 0 \cos\alpha & \sin\alpha \sin\beta \\ 1 & 0 & \cos\beta \end{bmatrix}, \ \boldsymbol{\Omega} \triangleq \begin{bmatrix} \dot{\alpha} \\ \dot{\beta} \\ \dot{\gamma} \end{bmatrix}$$
(4)

Assuming a slender stick, the moment of inertia matrix **J** in the inertial reference frame is related to the inertia matrix \mathbf{J}_b in the body-fixed $x_3y_3z_3$ frame by the expression

$$\mathbf{J} = \mathbf{R} \mathbf{J}_{b} \mathbf{R}^{\mathrm{T}}, \qquad \mathbf{J}_{b} \triangleq \operatorname{diag} \left[J \ J \ 0 \right]$$
 (5)

where the mass moment of inertia about the principal axis z_3 is zero. The matrix **J** is found to be independent of γ ; this is due to the symmetry of the stick about the z_3 - axis. Using (4), the angular momentum of the stick in the inertial reference frame, $\mathbf{H} \triangleq \begin{bmatrix} H_x & H_y & H_z \end{bmatrix}^T$, can be expressed as



where

$$\mathbf{JS} = J \begin{bmatrix} -\cos\alpha \sin\beta \cos\beta - \sin\alpha & 0 \\ -\sin\alpha \sin\beta \cos\beta & \cos\alpha & 0 \\ \sin^2\beta & 0 & 0 \end{bmatrix}$$
(7)

The above expression, which was obtained using (4) and (5), indicates that the matrix **JS** is singular and **H** is a function of $\dot{\alpha}$ and $\dot{\beta}$, but not $\dot{\gamma}$.

3.2 Impulsive dynamics

Let t_k , $k = 1, 2, \ldots$, denote the instants of time when impulsive inputs are applied on the stick. Furthermore, let t_k^- and t_k^+ denote the instants of time immediately before and after application of the impulsive inputs. Since impulsive inputs cause no change in position coordinates [2,11], we have

$$\mathbf{h}(t_k^+) = \mathbf{h}(t_k^-)$$

$$\alpha(t_k^+) = \alpha(t_k^-) \triangleq \alpha_k, \quad \beta(t_k^+) = \beta(t_k^-) = \beta^*$$
(8)

where α_k is defined for notational simplicity and $\beta(t_k^+) = \beta(t_k^-) = \beta^* \, \forall \, k$ follows from our discussion in Sect. 2. At time t_k , the vector of impulsive force can be written in the inertial reference frame as

$$\mathbf{I}_{k} = \mathbf{R}_{z}(\alpha_{k})\mathbf{R}_{y}(\beta^{*}) \begin{bmatrix} -I_{k}\cos\phi_{k} \\ -I_{k}\sin\phi_{k} \\ 0 \end{bmatrix} = I_{k}\mathbf{f}_{k},$$

$$\mathbf{f}_{k} \triangleq \begin{bmatrix} \sin\alpha_{k}\sin\phi_{k} - \cos\alpha_{k}\cos\beta^{*}\cos\phi_{k} \\ -\cos\alpha_{k}\sin\phi_{k} - \sin\alpha_{k}\cos\beta^{*}\cos\phi_{k} \\ \sin\beta^{*}\cos\phi_{k} \end{bmatrix}$$
(9)

where $I_k = I(t_k)$ and $\phi_k = \phi(t_k)$. The vector from the center-of-mass G to the point of application of the impulsive force can be written in the inertial reference frame as

$$\mathbf{r}_{k} = \mathbf{R}_{z}(\alpha_{k})\mathbf{R}_{y}(\beta^{*})\begin{bmatrix}0\\0\\r_{k}\end{bmatrix} = r_{k}\begin{bmatrix}\cos\alpha_{k}\sin\beta^{*}\\\sin\alpha_{k}\sin\beta^{*}\\\cos\beta^{*}\end{bmatrix}$$
(10)

where $r_k = r(t_k)$. The discontinuous jumps in velocities due to the impulsive inputs can be obtained from the linear and angular impulse-momentum relationships. The linear impulse-momentum relationship is given by

$$m\mathbf{v}(t_k^+) = m\mathbf{v}(t_k^-) + \mathbf{I}_k \tag{11}$$

which, using (9), can be expressed as

$$\mathbf{v}(t_k^+) = \mathbf{v}(t_k^-) + \frac{I_k}{m} \mathbf{f}_k \tag{12}$$



The angular impulse-momentum relationship is given by

$$\mathbf{H}(t_k^+) = \mathbf{H}(t_k^-) + \mathbf{r}_k \times \mathbf{I}_k \tag{13}$$

Using (6), (9), and (10), we get

$$\mathbf{J}_{k}\mathbf{S}_{k}\mathbf{\Omega}(t_{k}^{+}) = \mathbf{J}_{k}\mathbf{S}_{k}\mathbf{\Omega}(t_{k}^{-}) + I_{k}r_{k}$$

$$\times \begin{bmatrix} \sin\alpha_{k}\cos\phi_{k} + \cos\alpha_{k}\cos\beta^{*}\sin\phi_{k} \\ -\cos\alpha_{k}\cos\phi_{k} + \sin\alpha_{k}\cos\beta^{*}\sin\phi_{k} \\ -\sin\beta^{*}\sin\phi_{k} \end{bmatrix}$$
(14)

where $\mathbf{J}_k \mathbf{S}_k = \mathbf{J}(t_k) \mathbf{S}(t_k)$, and is obtained from (7) by using $\alpha = \alpha_k$ and $\beta = \beta^*$. It can be shown that two of the three equations in (14) are independent; these two equations can be used to solve for the two unknowns, namely,

$$\dot{\alpha}(t_k^+) = \dot{\alpha}(t_k^-) - \frac{I_k r_k \sin \phi_k}{J \sin \beta^*}$$
 (15a)

$$\dot{\beta}(t_k^+) = \dot{\beta}(t_k^-) - \frac{I_k r_k \cos \phi_k}{J}$$
 (15b)

Remark 1 The problem definition imposes the unilateral constraint

$$\beta \le \beta^* \quad \Rightarrow \quad \dot{\beta}(t_k^+) < 0 \quad \Rightarrow \quad r_k > 0$$
 (16)

Remark 2 The equations describing the impulsive dynamics are independent of γ and $\dot{\gamma}$.

3.3 Continuous-time dynamics

Over the interval $t \in [t_k^+, t_{k+1}^-]$, the stick undergoes torque-free motion under gravity. The motion of the center-of-mass is therefore described by the differential equation

$$\dot{\mathbf{h}} = \mathbf{v}, \qquad \dot{\mathbf{v}} = \begin{bmatrix} 0 \ 0 \ -g \end{bmatrix}^{\mathrm{T}} \tag{17}$$

Using $\mathbf{h}(t_k^+)$ and $\mathbf{v}(t_k^+)$ as the initial conditions for \mathbf{h} and \mathbf{v} , the solution to (17) is obtained as

$$\mathbf{h}(t_{k+1}^{-}) = \mathbf{h}(t_{k}^{-}) + \mathbf{v}(t_{k}^{-})\delta_{k} + \frac{I_{k}\delta_{k}}{m}\mathbf{f}_{k} - \frac{1}{2} \begin{bmatrix} 0\\0\\g\delta_{k}^{2} \end{bmatrix}$$
(18a)

$$\mathbf{v}(t_{k+1}^{-}) = \mathbf{v}(t_{k}^{-}) + \frac{I_{k}}{m}\mathbf{f}_{k} - \begin{bmatrix} 0\\0\\g\delta_{k} \end{bmatrix}$$
 (18b)

where $\delta_k \triangleq (t_{k+1}^- - t_k^-)$ is the interval between the kth and (k+1)th impulsive input; it is also the duration of the flight phase. Due to conservation of angular momentum, the rotational dynamics is described by the relation

$$\mathbf{H} = \mathbf{H}(t_k^+) \quad \Rightarrow \quad \mathbf{JS}\mathbf{\Omega} = \mathbf{H}(t_k^+)$$
 (19)

Since **JS** is singular, (19) yields the following three equations that are not all independent

$$J\dot{\alpha}\sin\beta\cos\beta = -H_x(t_k^+)\cos\alpha - H_y(t_k^+)\sin\alpha$$
(20a)

$$J\dot{\beta} = -H_x(t_k^+)\sin\alpha + H_y(t_k^+)\cos\alpha \tag{20b}$$

$$J\dot{\alpha}\sin^2\beta = H_z(t_\nu^+) \tag{20c}$$

where $H_x(t_k^+)$, $H_y(t_k^+)$, and $H_z(t_k^+)$ are the components of $\mathbf{H}(t_k^+)$, which can be obtained from (13). We now solve for α , $\dot{\alpha}$ and $\dot{\beta}$ at t_{k+1}^- , knowing that $\beta=\beta^*$ at t_{k+1}^- , which is the end of the flight phase. Eliminating $\dot{\alpha}$ between (20a) and (20c) and noting that $\beta=\beta^*$ both at the beginning and end of the flight phase, we get

$$H_{x}(t_{k}^{+})\cos\alpha_{k+1} + H_{y}(t_{k}^{+})\sin\alpha_{k+1} = H_{x}(t_{k}^{+})\cos\alpha_{k} + H_{y}(t_{k}^{+})\sin\alpha_{k}$$
 (21)

By ignoring the trivial solution $\alpha_{k+1} = \alpha_k$, we get

$$\alpha_{k+1} = \alpha_k + \pi + 2 \arctan$$

$$\left[\sin \beta^* \cos \beta^* \frac{\dot{\alpha}(t_k^-) - \frac{I_k r_k \sin \phi_k}{J \sin \beta^*}}{\dot{\beta}(t_k^-) - \frac{I_k r_k \cos \phi_k}{J}} \right]$$
(22)

Equation (20c) can be solved for $\dot{\alpha}(t_{k+1}^-)$ to obtain

$$\dot{\alpha}(t_{k+1}^{-}) = \dot{\alpha}(t_k^{-}) - \frac{I_k r_k \sin \phi_k}{J \sin \beta^*}$$
(23)

Differentiating (20b) with respect to time and eliminating terms in α and $\dot{\alpha}$ using (20a) and (20c) allows us to obtain a decoupled second-order differential equation in β :

$$J\ddot{\beta} = H_z^2(t_k^+) \cot \beta \csc^2 \beta$$

$$\Rightarrow J\dot{\beta}d\dot{\beta} = H_z^2(t_k^+) \cot \beta \csc^2 \beta d\beta$$
 (24)

The above equation can be integrated subject to initial conditions $\dot{\beta} = \dot{\beta}(t_k^+)$ and $\beta = \beta^*$ to obtain

$$\dot{\beta}^2 = -K_1 \cot^2 \beta + K_2 \tag{25}$$



where K_1 and K_2 are constants over the duration of the flight phase and are given by the relations

$$K_{1} \triangleq \sin^{4}\beta^{*} \left[\dot{\alpha}(t_{k}^{-}) - \frac{I_{k}r_{k}\sin\phi_{k}}{J\sin\beta^{*}} \right]^{2}$$

$$K_{2} \triangleq \sin^{2}\beta^{*}\cos^{2}\beta^{*} \left[\dot{\alpha}(t_{k}^{-}) - \frac{I_{k}r_{k}\sin\phi_{k}}{J\sin\beta^{*}} \right]^{2}$$

$$+ \left[\dot{\beta}(t_{k}^{-}) - \frac{I_{k}r_{k}\cos\phi_{k}}{J} \right]^{2}$$

$$(26)$$

To obtain $\dot{\beta}(t_{k+1}^-)$, we substitute $\beta = \beta^*$ in (25) and simplify. Since $\beta = \beta^*$ both at the beginning and end of the flight phase, we get two solutions. One solution gives the value of $\dot{\beta}$ at the beginning of the flight phase and is identical to (15b); the other gives the value of $\dot{\beta}$ at the end of the flight phase:

$$\dot{\beta}(t_{k+1}^{-}) = -\dot{\beta}(t_{k}^{-}) + \frac{I_{k}r_{k}\cos\phi_{k}}{J}$$
 (27)

To obtain the minimum value of β during the flight phase, we substitute $\dot{\beta} = 0$ in (25); this yields:

$$\beta_{\min} = \operatorname{arccot}\sqrt{K_2/K_1} \tag{28}$$

Separating the variables β and t in (25), and observing that $\dot{\beta}$ is necessarily negative (positive) when β changes from β^* to β_{\min} (β_{\min} to β^*), we obtain the time of flight δ_k as

$$\delta_{k} = \int_{\beta^{*}}^{\beta_{\min}} \frac{d\beta}{-\sqrt{K_{2} - K_{1} \cot^{2} \beta}} + \int_{\beta_{\min}}^{\beta^{*}} \frac{d\beta}{\sqrt{K_{2} - K_{1} \cot^{2} \beta}}$$

$$= 2 \int_{\beta_{\min}}^{\beta^{*}} \frac{d\beta}{\sqrt{K_{2} - K_{1} \cot^{2} \beta}}$$

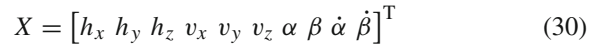
$$= \frac{1}{\sqrt{K_{1} + K_{2}}} \left[\pi - 2 \arctan\left(\frac{\sqrt{K_{1} + K_{2}} \cot \beta^{*}}{\sqrt{K_{2} - K_{1} \cot^{2} \beta^{*}}}\right) \right]$$
(29)

Remark 3 Similar to the impulsive dynamics, the equations describing the continuous-time dynamics are independent of γ and $\dot{\gamma}$. Therefore, the configuration of the stick can be adequately described by the five generalized coordinates $(h_x, h_y, h_z, \alpha, \beta)$.

4 Hybrid dynamic model

4.1 Poincaré map in inertial reference frame

In light of Remark 3, the generalized coordinates and their derivatives can be chosen to be the components of the state vector:



The vector of control inputs is denoted by

$$U = \begin{bmatrix} I & r & \phi \end{bmatrix}^{\mathrm{T}} \tag{31}$$

We now define the Poincaré section¹ based on the configuration where the impulsive inputs are applied:

$$S = \{ X \in \mathbb{R}^{10} \mid \beta = \beta^* \} \tag{32}$$

A point on *S* can be described by the vector Y, $Y \subset X$, where

$$Y = \left[h_x \ h_y \ h_z \ v_x \ v_y \ v_z \ \alpha \ \dot{\alpha} \ \dot{\beta} \right]^{\mathrm{T}}$$
 (33)

Using (18), (22), (23) and (27), the hybrid dynamics, comprised of the impulsive and continuous-time dynamics, can be described by the map $\mathbb{P}: S \to S$ as follows:

$$Y(t_{k+1}^{-}) = \mathbb{P}[Y(t_{k}^{-}), U_{k}]$$

$$= \begin{bmatrix} h_{x}(t_{k}^{-}) + v_{x}(t_{k}^{-})\delta_{k} + \frac{I_{k}\delta_{k}}{m}(\sin\alpha_{k}\sin\phi_{k} \\ -\cos\alpha_{k}\cos\beta^{*}\cos\phi_{k}) \end{bmatrix}$$

$$h_{y}(t_{k}^{-}) + v_{y}(t_{k}^{-})\delta_{k} + \frac{I_{k}\delta_{k}}{m}(-\cos\alpha_{k}\sin\phi_{k} \\ -\sin\alpha_{k}\cos\beta^{*}\cos\phi_{k}) \end{bmatrix}$$

$$h_{z}(t_{k}^{-}) + v_{z}(t_{k}^{-})\delta_{k} + \frac{I_{k}\delta_{k}}{m}\sin\beta^{*}\cos\phi_{k} \\ -\frac{1}{2}g\delta_{k}^{2} \end{bmatrix}$$

$$v_{x}(t_{k}^{-}) + \frac{I_{k}}{m}(\sin\alpha_{k}\sin\phi_{k} \\ -\cos\alpha_{k}\cos\beta^{*}\cos\phi_{k}) \end{bmatrix}$$

$$v_{y}(t_{k}^{-}) + \frac{I_{k}}{m}(-\cos\alpha_{k}\sin\phi_{k} \\ -\sin\alpha_{k}\cos\beta^{*}\cos\phi_{k}) \end{bmatrix}$$

$$v_{z}(t_{k}^{-}) + \frac{I_{k}}{m}\sin\beta^{*}\cos\phi_{k} - g\delta_{k}$$

$$\alpha_{k} + \pi + 2$$

$$\times \arctan\left[\sin\beta^{*}\cos\beta^{*}\frac{\dot{\alpha}(t_{k}^{-}) - \frac{I_{k}r_{k}\sin\phi_{k}}{J\sin\beta^{*}}}{\dot{\beta}(t_{k}^{-}) - \frac{I_{k}r_{k}\cos\phi_{k}}{J}}\right]$$

$$\dot{\alpha}(t_{k}^{-}) - \frac{I_{k}r_{k}\sin\phi_{k}}{J\sin\beta^{*}}$$

$$-\dot{\beta}(t_{k}^{-}) + \frac{I_{k}r_{k}\cos\phi_{k}}{J}$$

$$(34)$$



¹ It is assumed that the initial conditions of the stick are such that its trajectory intersects the Poincaré section before the first impulsive input is applied.

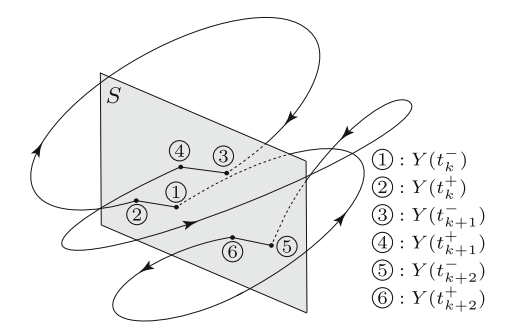


Fig. 4 Steady-state trajectory of the stick in the inertial reference frame for the particular case of $\Delta \alpha^* = 2\pi/3$; starting from the configuration ①: $Y(t_k^-)$, the stick returns to this configuration at t_{k+3}^- following the application of three control actions at t_k , t_{k+1} , and t_{k+2}

Remark 4 All elements of the vector Y in (34) are defined in the inertial reference frame.

Remark 5 The objective is to juggle the stick between a sequence of configurations which are rotationally symmetric about the z-axis at steady-state—see problem description in Sect. 2. These steady-state configurations do not correspond to a fixed point of the map \mathbb{P} in (34) since each variable in the set $\{h_x, h_y, v_x, v_y, \alpha\}$ does not converge to a fixed value. This is illustrated with the help of Fig. 4, which shows the Poincaré section S and the steady-state trajectory of the stick for the particular case of $\Delta \alpha^* = 2\pi/3$. The stick is juggled between three configurations that are rotationally symmetric about the vertical axis and three control actions are required to bring the stick back to the original configuration, i.e., $Y(t_{k+3}^-) = Y(t_k^-)$. The impulsive dynamics of the stick is shown by the line segments $(1) \rightarrow (2)$, $(3) \rightarrow (4)$, and $(5) \rightarrow (6)$ on S; the continuoustime dynamics is shown by the trajectories $(2) \rightarrow (3)$, $4 \rightarrow 5$, and $6 \rightarrow 1$. It can be seen that the steadystate configurations $Y(t_k^-)$, $Y(t_{k+1}^-)$, and $Y(t_{k+2}^-)$ are different in the inertial coordinate system and do not correspond to a fixed point of \mathbb{P} . This problem can be alleviated by defining the map in a rotating reference frame following the approach in [9].

4.2 Poincaré map in the reference frame of the juggler

We assume that the juggler changes its position intermittently. This position, which is denoted by P, is updated immediately prior to application of each impulsive input, *i.e.*, when $\beta = \beta^*$. The point P lies on a circle whose center is the origin of the xyz frame O, and OP is parallel to the x_1 -axis at instants $t = t_k$,

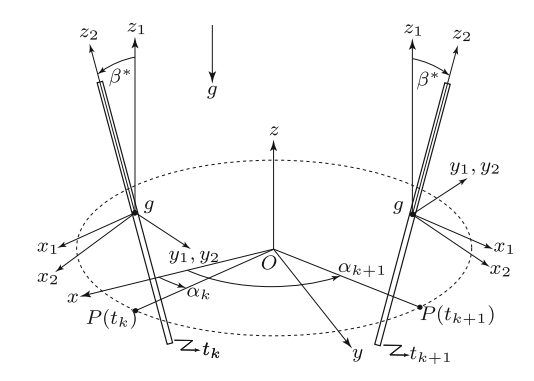


Fig. 5 Configurations of the stick at t_k and t_{k+1} ; the locations of the juggler are denoted by $P(t_k)$ and $P(t_{k+1})$

 $k=1,2,\ldots$ The reference frame of the juggler is obtained by rotating the xyz frame intermittently by α_k at $t=t_k^-, k=1,2,\ldots$, about the z-axis; this frame remains stationary in the interval $[t_k,t_{k+1}^-)$. The configurations of the stick and locations of P at instants t_k and t_{k+1} are shown in Fig. 5. We denote the position and velocity of the center-of-mass of the stick in the reference frame of the juggler by the vectors $\bar{\mathbf{h}}$ and $\bar{\mathbf{v}}$. Noting that $\alpha=\alpha_k$ at t_k^- and $\alpha=\alpha_{k+1}$ at t_{k+1}^- , (18) can be written as

$$\mathbf{R}_{z}(\alpha_{k+1})\bar{\mathbf{h}}(t_{k+1}^{-}) = \mathbf{R}_{z}(\alpha_{k})\bar{\mathbf{h}}(t_{k}^{-}) + \mathbf{R}_{z}(\alpha_{k})\bar{\mathbf{v}}(t_{k}^{-})\delta_{k}$$

$$+ \frac{I_{k}\delta_{k}}{m}\mathbf{f}_{k} - \frac{1}{2}\begin{bmatrix}0\\0\\g\delta_{k}^{2}\end{bmatrix}$$
(35a)

$$\mathbf{R}_{z}(\alpha_{k+1})\bar{\mathbf{v}}(t_{k+1}^{-}) = \mathbf{R}_{z}(\alpha_{k})\bar{\mathbf{v}}(t_{k}^{-}) + \frac{I_{k}}{m}\mathbf{f}_{k} - \begin{bmatrix} 0\\0\\g\delta_{k} \end{bmatrix}$$
(35b)

Premultiplying both sides of (35) by $\mathbf{R}_z^{\mathrm{T}}(\alpha_k)$ and using the identity

$$\mathbf{R}_{z}^{\mathrm{T}}(\alpha_{k})\mathbf{R}_{z}(\alpha_{k+1}) = \mathbf{R}_{z}(\Delta\alpha_{k})$$

$$\Delta\alpha_{k} \triangleq (\alpha_{k+1} - \alpha_{k})$$
(36)

we get

$$\bar{\mathbf{h}}(t_{k+1}^{-}) = \mathbf{R}_{z}^{\mathrm{T}}(\Delta \alpha_{k}) \left\{ \bar{\mathbf{h}}(t_{k}^{-}) + \bar{\mathbf{v}}(t_{k}^{-}) \delta_{k} + \frac{I_{k} \delta_{k}}{m} \bar{\mathbf{f}}_{k} - \frac{1}{2} \begin{bmatrix} 0\\0\\g \delta_{k}^{2} \end{bmatrix} \right\}$$
(37a)



$$\bar{\mathbf{v}}(t_{k+1}^{-}) = \mathbf{R}_{z}^{\mathrm{T}}(\Delta \alpha_{k}) \left\{ \bar{\mathbf{v}}(t_{k}^{-}) + \frac{I_{k}}{m} \bar{\mathbf{f}}_{k} - \begin{bmatrix} 0\\0\\g\delta_{k} \end{bmatrix} \right\}$$
(37b)

where

$$\bar{\mathbf{f}}_{k} \triangleq \mathbf{R}_{z}^{\mathrm{T}}(\alpha_{k})\mathbf{f}_{k} = \begin{bmatrix} -\cos\beta^{*}\cos\phi_{k} \\ -\sin\phi_{k} \\ \sin\beta^{*}\cos\phi_{k} \end{bmatrix}$$

$$\Delta\alpha_{k} = \pi + 2\arctan\left[\sin\beta^{*}\cos\beta^{*} \frac{\dot{\alpha}(t_{k}^{-}) - \frac{I_{k}r_{k}\sin\phi_{k}}{J\sin\beta^{*}}}{\dot{\beta}(t_{k}^{-}) - \frac{I_{k}r_{k}\cos\phi_{k}}{J}}\right]$$
(38)

$$\bar{S} = \{ \bar{X} \in \mathbb{R}^9 \mid \beta = \beta^* \} \tag{40}$$

A point on \bar{S} can be described by the vector \bar{Y} , $\bar{Y} \subset \bar{X}$, where

$$\bar{Y} = \left[\bar{h}_x \ \bar{h}_y \ \bar{h}_z \ \bar{v}_x \ \bar{v}_y \ \bar{v}_z \ \dot{\alpha} \ \dot{\beta}\right]^{\mathrm{T}}$$
 (41)

Using (23), (27), and (37), the map $\overline{\mathbb{P}}: \overline{S} \to \overline{S}$ can be expressed in the reference frame of the juggler as

$$\begin{split} \bar{Y}(t_{k+1}^-) &= \bar{\mathbb{P}}\left[\bar{Y}(t_k^-), U_k\right] \triangleq \mathcal{R}^{\mathrm{T}}(\Delta\alpha_k) \,\mathcal{F}\left[\bar{Y}(t_k^-), U_k\right] \\ & \begin{bmatrix} \bar{h}_x(t_k^-) + \bar{v}_x(t_k^-) \delta_k - \frac{I_k \delta_k}{m} \cos \beta^* \cos \phi_k \\ \bar{h}_y(t_k^-) + \bar{v}_y(t_k^-) \delta_k - \frac{I_k \delta_k}{m} \sin \phi_k \\ \bar{h}_z(t_k^-) + \bar{v}_z(t_k^-) \delta_k + \frac{I_k \delta_k}{m} \sin \beta^* \cos \phi_k \\ & - \frac{1}{2} g \delta_k^2 \\ \\ \bar{v}_x(t_k^-) - \frac{I_k}{m} \cos \beta^* \cos \phi_k \\ \bar{v}_y(t_k^-) - \frac{I_k}{m} \sin \phi_k \\ \bar{v}_z(t_k^-) + \frac{I_k}{m} \sin \beta^* \cos \phi_k - g \delta_k \\ & \dot{\alpha}(t_k^-) - \frac{I_k r_k \sin \phi_k}{J \sin \beta^*} \\ & - \dot{\beta}(t_k^-) + \frac{I_k r_k \cos \phi_k}{J} \end{bmatrix} \end{split}, \quad \mathcal{R}(\Delta\alpha_k) \triangleq \begin{bmatrix} \mathbf{R}_z(\Delta\alpha_k) & \mathbb{O}_{3\times 3} & \mathbb{O}_{3\times 2} \\ \mathbb{O}_{3\times 3} & \mathbb{R}_z(\Delta\alpha_k) & \mathbb{O}_{3\times 2} \\ \mathbb{O}_{2\times 3} & \mathbb{O}_{2\times 3} & \mathbb{O}_{2\times 3} \end{bmatrix} \end{split}$$

$$\mathcal{R}(\Delta \alpha_k) \triangleq \begin{bmatrix} \mathbf{R}_z(\Delta \alpha_k) & \mathbb{O}_{3 \times 3} & \mathbb{O}_{3 \times 2} \\ \mathbb{O}_{3 \times 3} & \mathbf{R}_z(\Delta \alpha_k) & \mathbb{O}_{3 \times 2} \\ \mathbb{O}_{2 \times 3} & \mathbb{O}_{2 \times 3} & \mathbb{I}_{2 \times 2} \end{bmatrix}$$

(42)

The above expression for $\Delta \alpha_k$ was obtained from (22).

Based on the description of the reference frame of the juggler, it is clear that the juggler is unaware of the value of α but aware of the values of $\dot{\alpha}$, β and $\dot{\beta}$. Therefore, in this reference frame, the state vector is

$$\bar{X} = \left[\bar{h}_x \ \bar{h}_y \ \bar{h}_z \ \bar{v}_x \ \bar{v}_y \ \bar{v}_z \ \beta \ \dot{\alpha} \ \dot{\beta}\right]^{\mathrm{T}}$$
(39)

Similar to (32), the Poincaré section in the reference frame of the juggler is defined as:

where $\Delta \alpha_k$ is given by (38), $\mathbb{O}_{m \times n} \in \mathbb{R}^{m \times n}$ is a matrix of zeros and $\mathbb{I}_{n\times n}\in\mathbb{R}^{n\times n}$ is the identity matrix.

Remark 6 A sequence of configurations which are rotationally symmetric about the z-axis at steady-state (see Remark 5) corresponds to a fixed configuration in the reference frame of the juggler. This configuration corresponds to a fixed point of the map $\bar{\mathbb{P}}$ in (42). Indeed, unlike \mathbb{P} , $\overline{\mathbb{P}}$ is not a function of variables in the set $\{h_x, h_y, v_x, v_y, \alpha\}$. The steady-state trajectory of the stick in the reference frame of the juggler is shown in red in Fig. 6.



5 Control design for juggling

5.1 Steady-state dynamics

The objective of juggling the stick between a sequence of rotationally symmetric configurations is equivalent to finding a fixed point of the Poincaré map in (42), defined in the reference frame of the juggler. A fixed point of the map $\bar{\mathbb{P}}$ is given by the pair $\{\bar{Y}^*, U^*\}$ which satisfies

$$\bar{Y}^* = \bar{\mathbb{P}}(\bar{Y}^*, U^*)
\bar{Y}^* \triangleq \left[\bar{h}_x^* \, \bar{h}_y^* \, \bar{h}_z^* \, \bar{v}_x^* \, \bar{v}_y^* \, \bar{v}_z^* \, \dot{\alpha}^* \, \dot{\beta}^*\right]^{\mathrm{T}}
U^* \triangleq \left[I^* \, r^* \, \phi^*\right]^{\mathrm{T}}$$
(43)

subject to the expressions that follow from (29) and (38):

$$\delta^* = \frac{1}{\sqrt{K_1^* + K_2^*}} \times \left[\pi - 2 \arctan\left(\frac{\sqrt{K_1^* + K_2^*} \cot \beta^*}{\sqrt{K_2^* - K_1^* \cot^2 \beta^*}}\right) \right]$$
(44)

 $\Delta \alpha^* = \pi + 2 \arctan$

$$\begin{bmatrix}
\sin \beta^* \cos \beta^* \frac{\dot{\alpha}^* - \frac{I^* r^* \sin \phi^*}{J \sin \beta^*}}{\dot{\beta}^* - \frac{I^* r^* \cos \phi^*}{J}}
\end{bmatrix} \tag{45}$$

where

$$K_{1}^{*} = \sin^{4}\beta^{*} \left[\dot{\alpha}^{*} - \frac{I^{*}r^{*}\sin\phi^{*}}{J\sin\beta^{*}} \right]^{2}$$

$$K_{2}^{*} = \sin^{2}\beta^{*}\cos^{2}\beta^{*} \left[\dot{\alpha}^{*} - \frac{I^{*}r^{*}\sin\phi^{*}}{J\sin\beta^{*}} \right]^{2}$$

$$+ \left[\dot{\beta}^{*} - \frac{I^{*}r^{*}\cos\phi^{*}}{J} \right]^{2}$$
(46)

The relations in (43), (44) and (45) represent 10 equations in 13 unknowns, namely $\bar{h}_x^*, \bar{h}_y^*, \bar{h}_z^*, \bar{v}_x^*, \bar{v}_y^*, \bar{v}_z^*, \dot{\alpha}^*, \dot{\beta}^*, I^*, r^*, \phi^*, \delta^*$, and $\Delta \alpha^*$. The unknown \bar{h}_z^* is eliminated after simplification of (43); this leaves us with

10 equations in 12 unknowns. We choose the values of δ^* and $\Delta \alpha^*$ to solve for the remaining ten unknowns:

$$\begin{split} \bar{h}_x^* &= \frac{g \delta^{*2} \cot \beta^*}{2(1 - \cos \Delta \alpha^*)}, \quad \bar{h}_y^* = 0 \\ \bar{v}_x^* &= \frac{g \delta^* \cot \beta^*}{2}, \qquad \bar{v}_y^* = \frac{g \delta^* \cot \beta^* \sin \Delta \alpha^*}{2(1 - \cos \Delta \alpha^*)} \\ \bar{v}_z^* &= -\frac{1}{2} g \delta^*, \qquad \dot{\alpha}^* = \frac{\Psi \sin \Delta \alpha^*}{\delta^* \sin 2\beta^* (1 - \cos \Delta \alpha^*)} \\ \dot{\beta}^* &= \frac{\Psi}{2\delta^*}, \qquad I^* &= \frac{mg \delta^*}{\sin \beta^*} \\ r^* &= \frac{J\Psi \sin \beta^*}{mg \delta^{*2}}, \qquad \phi^* &= 0 \end{split}$$

where

$$\Psi = \frac{2}{\xi} \left[\pi - 2 \arctan \left(\xi \cot \beta^* \right) \right]$$

$$\xi \triangleq \sqrt{1 + \sec^2 \beta^* \left[\frac{\sin \Delta \alpha^*}{1 - \cos \Delta \alpha^*} \right]^2}$$
(48)

The value $\bar{h}_y^* = 0$ indicates that, at steady-state, the stick lies in the vertical plane containing point P at instants when impulsive inputs are applied; $\phi^* = 0$ indicates that, at steady-state, the impulsive force vector also lies in this plane. The point of application of the impulsive force must lie on the stick, *i.e.*, $0 \le r^* \le \ell/2$; this imposes the following constraint on the time of flight:

$$\delta^* = p \, \delta_{\min}, \quad \delta_{\min} \triangleq \sqrt{\frac{2J\Psi \sin \beta^*}{mg\ell}}, \quad p \ge 1$$
 (49)

The above relation requires that $\Psi \geq 0$. Without loss of generality, we assume that $\dot{\alpha}^* > 0$, *i.e.*, the stick is juggled between a sequence of configurations where one configuration is obtained from the previous by a counterclockwise rotation about the z-axis; from the expression of $\dot{\alpha}^*$ in (47), the choice of $\Delta \alpha^*$ must satisfy $\Delta \alpha^* \in (0, \pi]$.

The desired juggling motion of the stick is repetitive in nature and can be described by the following hybrid orbit:

$$\bar{\mathcal{O}}^* = \{ \bar{X} \in \mathbb{R}^9 \mid \bar{Y}(t_k^-) = \bar{Y}^*, U_k = U^* \}$$
 (50)

In the next subsection, we address the problem of stabilization of the hybrid orbit $\bar{\mathcal{O}}^*$, which is equivalent to stabilization of desired juggling motion.



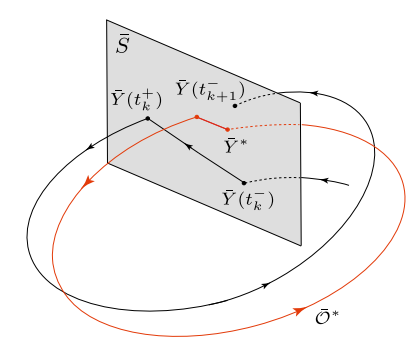


Fig. 6 Schematic of the ICPM approach to hybrid orbit stabilization. The steady-state orbit of the stick in the reference frame of the juggler is shown in red

5.2 Hybrid orbit stabilization

In the absence of disturbances, the input vector U^* in (43) ensures desired juggling motion if $\bar{Y}(t_k^-) = \bar{Y}^*$. However, if this is not the case, the trajectory of the stick may not converge to the desired orbit $\bar{\mathcal{O}}^*$ with input U^* . It is therefore necessary to determine the stability characteristics of $\bar{\mathcal{O}}^*$. To this end, we define an ϵ -neighborhood of $\bar{\mathcal{O}}^*$ as follows:

$$N_{\epsilon} = \{ \bar{X} \in \mathbb{R}^9 : \operatorname{dist}(\bar{X}, \bar{\mathcal{O}}^*) < \epsilon \}$$

$$\operatorname{dist}(\bar{X}, \bar{\mathcal{O}}^*) \triangleq \inf_{Z \in \bar{\mathcal{O}}^*} \|\bar{X} - Z\|$$

Definition 1 The orbit $\bar{\mathcal{O}}^*$ in (50) is

- stable, if for every $\epsilon > 0$, there is a $\delta > 0$ such that $\bar{X}(0) \in N_{\delta} \Rightarrow \bar{X}(t) \in N_{\epsilon}, \ \forall t \geq 0$.
- asymptotically stable if it is stable and δ can be chosen such that $\lim_{t\to\infty} \operatorname{dist}(\bar{X}(t), \bar{\mathcal{O}}^*) = 0$.

The hybrid orbit $\bar{\mathcal{O}}^*$ in (50) is asymptotically stable if the fixed point \bar{Y}^* in (43) is asymptotically stable [10, Th. 1], which is an abridged version of [7, Th. 1] and [19, Th. 2.1]. To stabilize the fixed point \bar{Y}^* , we use the Impulse Controlled Poincaré Map (ICPM) approach [8], which was developed for continuous orbits, and later extended to hybrid orbits associated with planar stick juggling [10]. The ICPM approach is explained with the help of Fig. 6. The desired hybrid orbit $\bar{\mathcal{O}}^*$ (shown in red), first intersects the Poincaré section \bar{S} at the fixed point \bar{Y}^* . It then undergoes a discontinuous jump due to application of the input U^* before exiting \bar{S} and evolving continuously. For a trajectory not on $\bar{\mathcal{O}}^*$ (shown in black), the configuration jumps from

 $\bar{Y}(t_k^-)$ to $\bar{Y}(t_k^+)$ on \bar{S} due to the application of input U_k . Hereafter, the stick undergoes torque free motion under gravity and the next intersection of the continuous-time trajectory with \bar{S} is denoted by $\bar{Y}(t_{k+1}^-)$.

To apply the ICPM approach, we linearize the Poincaré map $\bar{\mathbb{P}}$ in (42) about $\bar{Y} = \bar{Y}^*$ and $U = U^*$ as follows:

$$e(k+1) = \mathcal{A}e(k) + \mathcal{B}u(k)$$

$$e(k) \triangleq \bar{Y}(t_k^-) - \bar{Y}^*, \quad u(k) \triangleq U_k - U^*$$
(51)

where

$$\mathcal{A} \triangleq \left[\nabla_{\bar{Y}} \mathbb{P}(\bar{Y}, U)\right]_{\bar{Y} = \bar{Y}^*; U = U^*}$$

$$\mathcal{B} \triangleq \left[\nabla_U \mathbb{P}(\bar{Y}, U)\right]_{\bar{Y} = \bar{Y}^*; U = U^*}$$
(52)

The analytical expressions for \mathcal{A} and \mathcal{B} are not provided here for brevity. From the expressions, it can be verified that the pair $(\mathcal{A}, \mathcal{B})$ is controllable. The hybrid orbit $\bar{\mathcal{O}}^*$ can therefore be stabilized by the following discrete feedback:

$$u(k) = \mathcal{K}e(k) \tag{53}$$

where the matrix K is chosen such that the eigenvalues of (A + BK) lie inside the unit circle.

6 Simulation

The physical parameters of the stick in SI units are:

$$m = 0.1, \quad \ell = 0.5, \quad J = \frac{1}{12}m\ell^2 = 0.0021$$
 (54)

Choosing $\beta^* = \pi/3$ rad, $\delta^* = 0.6$ s, and $\Delta \alpha^* = 2\pi/3$ rad, and using (54) in (47), we obtain

$$\bar{h}_{x}^{*} = 0.6797 \text{ m}, \qquad \bar{h}_{y}^{*} = 0$$
 $\bar{v}_{x}^{*} = 1.6991 \text{ m/s}, \qquad \bar{v}_{y}^{*} = 0.9810 \text{ m/s}$
 $\bar{v}_{z}^{*} = -2.9430 \text{ m/s}, \qquad \dot{\alpha}^{*} = 2.4675 \text{ rad/s}$
 $\dot{\beta}^{*} = 1.8506 \text{ rad/s}, \qquad I^{*} = 0.6797 \text{ Ns}$
 $r^{*} = 0.0113 \text{ m}, \qquad \phi^{*} = 0$

The value \bar{h}_z^* is chosen arbitrarily to be 1.6 m.

The gain matrix K in (53), which is not provided here for brevity, is designed using the LQR method [1]; it minimizes the cost functional

$$\mathcal{J} = \sum_{k=1}^{\infty} \left[e(k)^{\mathrm{T}} Q e(k) + u(k)^{\mathrm{T}} R u(k) \right]$$



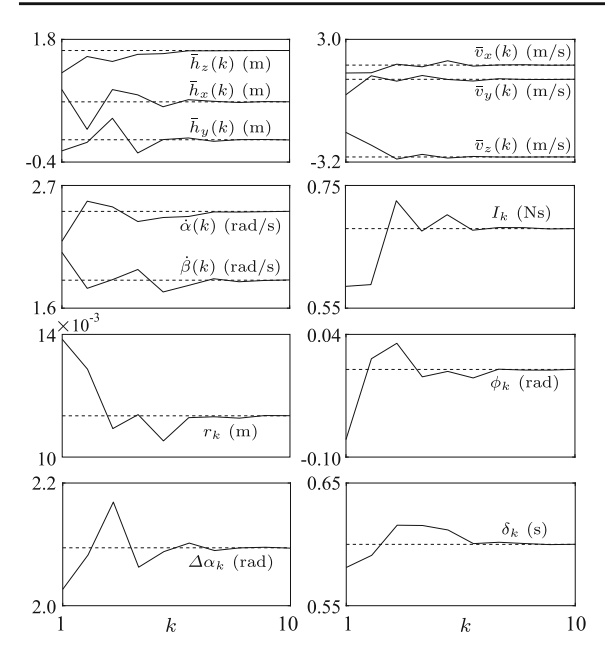


Fig. 7 Simulation results: the state variables, control inputs, precession $\Delta \alpha_k$, and time of flight δ_k are shown at time instants t_k^- , k = 1, 2, ..., 10, for the initial conditions in (57)

where the Q and R matrices were chosen as

$$Q = \mathbb{I}_{8 \times 8}, \quad R = \text{diag} [2.0 \ 0.5 \ 1.0]$$
 (56)

We assume that $\beta(1) = \beta^* = \pi/3$ rad and choose the initial values of the states as

$$\bar{h}_x(1) = 0.9 \text{ m}, \qquad \bar{h}_y(1) = -0.2 \text{ m}$$
 $\bar{h}_z(1) = 1.2 \text{ m}, \qquad \bar{v}_x(1) = 1.3 \text{ m/s}$
 $\bar{v}_y(1) = 0.2 \text{ m/s}, \qquad \bar{v}_z(1) = -1.7 \text{ m/s}$

$$\dot{\alpha}(1) = 2.2 \text{ rad/s}, \qquad \dot{\beta}(1) = 2.1 \text{ rad/s}$$
(57)

The simulation results are shown in Figs. 7 and 8. Figure 7 shows that the states and inputs converge to their steady-state values, indicated by dotted lines, in approx. k=10 steps. This validates that desired juggling motion of the stick is achieved through stabilization of the fixed point \bar{Y}^* . The trajectory of the center-of-mass of the stick over approx. 12.02 s (corresponding to k=20 steps) is shown in Fig. 8; a video of the juggling motion is uploaded as supplementary material.

Remark 7 At steady-state, the kinetic energy of the stick is the same before and after the application of each impulsive force; therefore, the impulsive forces do no work. Since the energy of the stick remains con-

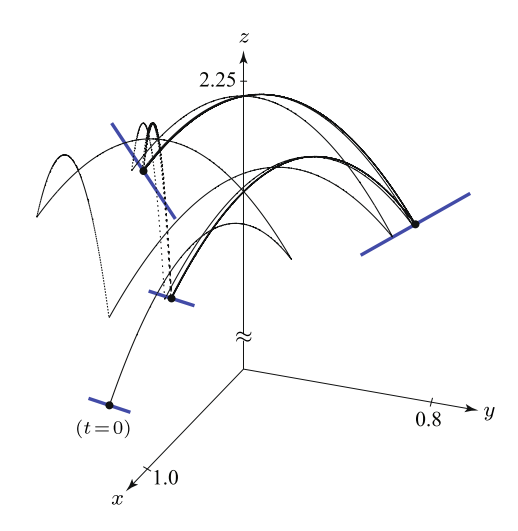


Fig. 8 Trajectory of the center-of-mass of the stick in the inertial frame; also shown is the stick in its initial configuration (t=0) and three rotationally symmetric steady-state configurations

stant during the flight phase, the mechanical energy of the stick is conserved at steady-state.

To demonstrate robustness of the closed-loop system to losses and uncertainties in the state measurements, we consider a random reduction in the magnitude of the impulsive force I_k in the range 0.0-2.5% of its computed value, random noise in the position measurements $\bar{h}_x(k)$, $\bar{h}_y(k)$, and $\bar{h}_z(k)$ in the range $\pm 1.0\%$, and random noise in the linear and angular velocity measurements $\bar{v}_x(k)$, $\bar{v}_y(k)$, $\bar{v}_z(k)$, $\dot{\alpha}(k)$, and $\dot{\beta}(k)$ in the range $\pm 2.5\%$. For the same parameter values in (54), steady-state values in (55), initial conditions in (57), and gain matrix K, the simulation results are shown in Fig. 9 for k = 40 steps. The results of the simulation, which was carried out for a much larger number of steps than shown, indicate that errors in the state variables, control inputs, precession angle, and time of flight remain bounded, implying stable behavior.

7 Special cases

7.1 Planar juggling

The choice $\Delta \alpha^* = \pi$ reduces the problem to that of planar symmetric juggling, which was discussed in [9, 10]. Setting $\Delta \alpha^* = \pi$ in (47) yields



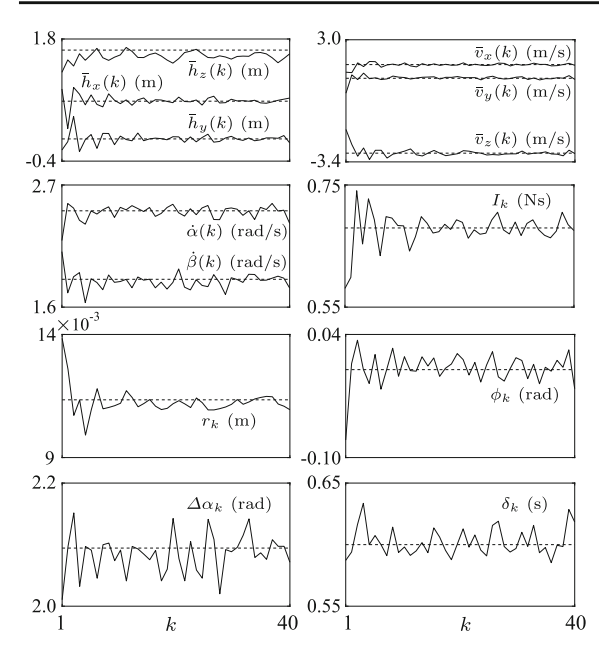


Fig. 9 Simulation results demonstrating stable behavior in the presence of energy losses: the state variables, control inputs, precession $\Delta \alpha_k$, and time of flight δ_k are shown at time instants t_k^- , $k=1,2,\ldots,40$, for the initial conditions in (57)

$$\begin{split} \bar{h}_{x}^{*} &= (g\delta^{*2}\cot\beta^{*})/4, & \bar{h}_{y}^{*} &= 0\\ \bar{v}_{x}^{*} &= (g\delta^{*}\cot\beta^{*})/2, & \bar{v}_{y}^{*} &= 0\\ \bar{v}_{z}^{*} &= -g\delta^{*}/2, & \dot{\alpha}^{*} &= 0\\ \dot{\beta}^{*} &= 2\beta^{*}/\delta^{*}, & I^{*} &= mg\delta^{*}/\sin\beta^{*}\\ r^{*} &= (4J\beta^{*}\sin\beta^{*})/mg\delta^{*2}, & \phi^{*} &= 0 \end{split}$$
(58)

which are identical to those derived in [9,10]. Compared to the results in [9,10], the current formulation is more general in that the initial condition can be arbitrary and need not be restricted to lie on the plane of steady juggling.

7.2 Steady precession

In the limiting case where $\Delta \alpha^* \to 0^+$, the surface traced by the motion of the stick defines an inverted cone of semi-vertex angle β^* —see Fig. 10. The discrete set of impulsive forces tend to a continuous force F^* that acts in the direction normal to the cone. The point of application of F^* lies at a distance of $r = r^*$ and traces a circle on the cone. This circle can be viewed as a hoop on which the stick slides without friction and precesses; F^* is the reaction force of the hoop on the stick. The center-of-mass G also traces a circle on

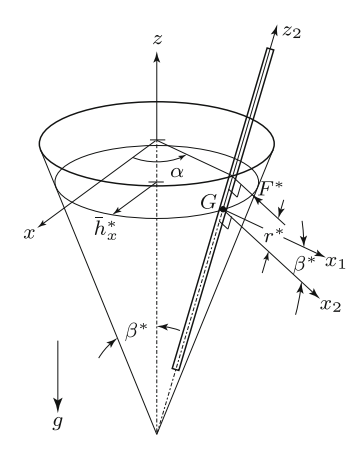


Fig. 10 Motion of stick in the limiting case of $\Delta \alpha^* \to 0^+$

the cone; the radius of this circle is \bar{h}_x^* . In the limit, the steady-state time of flight, which satisfies the constraint in (49), equals

$$\lim_{\Delta \alpha^* \to 0^+} \delta^* = p \lim_{\Delta \alpha^* \to 0^+} \delta_{\min} = 0$$
 (59)

The above result, which is intuitive, can be obtained from (49) by computing the value of Ψ in (48) in the limit $\Delta \alpha^* \to 0^+$. The continuous force F^* can be expressed by the relation

$$F^* = \frac{I^*}{\delta^*} \tag{60}$$

since the impulse of the force over the time interval δ^* , which is equal to $F^*\delta^*$, must equal the impulse I^* of the impulsive force at steady-state. By replacing the expression for I^* in (47) with F^* in (60) and taking the limit $\Delta\alpha^* \to 0^+$, we get the following values that describe the dynamics of the stick:

$$\begin{split} \bar{h}_{x}^{*} &= \frac{2p^{2}J\sin\beta^{*}\cos^{2}\beta^{*}}{m\ell}, \quad \bar{h}_{y}^{*} = 0 \\ \bar{v}_{x}^{*} &= 0, \qquad \qquad \bar{v}_{y}^{*} = p\sqrt{\frac{2Jg\cos^{3}\beta^{*}}{m\ell}} \\ \bar{v}_{z}^{*} &= 0, \qquad \qquad \dot{\alpha}^{*} = \frac{1}{p}\sqrt{\frac{mg\ell}{2J\sin^{2}\beta^{*}\cos\beta^{*}}} \\ \dot{\beta}^{*} &= 0, \qquad \qquad F^{*} = mg/\sin\beta^{*} \\ r^{*} &= \ell/(2p^{2}), \qquad \phi^{*} &= 0 \end{split}$$

In the above expressions, p is a free parameter. For a specific value of p, $p \ge 1$, the stick will exhibit a unique motion. The results in (61) can be independently derived (see "Appendix") by considering the continuous-time dynamics of the stick.



8 Conclusions

Juggling is an example of nonprehensile manipulation using intermittent impulsive forces. An experienced juggler can juggle a stick between desired configurations by intermittently applying impulsive forces while the stick falls freely under gravity. With the motivation of enabling robotic systems to perform complex nonprehensile manipulation tasks that can be performed by humans, the problem of juggling a stick in three-dimensional space is considered in this paper.

We consider juggling a stick between a sequence of configurations that are rotationally symmetric about the vertical axis. The stick is assumed to be slender and its configuration is described by five generalized coordinates. The location, direction, and magnitude of the impulsive forces applied on the stick are modeled as the control inputs. The control is event-based, with impulsive forces applied when the stick reaches a desired orientation relative to the vertical axis. The hybrid dynamics of the stick is represented using a Poincaré map but the sequence of rotationally symmetric configurations do not correspond to a fixed point of this map. To alleviate this problem, the Poincaré map is redefined in a rotating reference frame. The trajectory of the stick at steady-state is represented by a hybrid orbit, and stabilizing the desired juggling motion is equivalent to stabilization of the hybrid orbit; this is accomplished through stabilization of the fixed point of the Poincaré map in the rotating reference frame. Using the ICPM approach, the Poincaré map is linearized about the fixed point and this results in a controllable linear discrete-time system. Simulation results based on an LQR design are presented to demonstrate stabilization of a desired juggling motion from an arbitrary initial configuration.

In our approach, the angle of precession of the stick about the vertical axis between consecutive control actions at steady-state can be specified. When this angle equals π rad, the model for planar symmetric stick-juggling [9] is recovered. In the limiting case, when the angle approaches zero, the hybrid dynamics approaches the continuous-time dynamics of steady precession on a hoop. With focus on robotic juggling, our future work will extend the model presented here to include the mechanics of impact, address the motion planning and control problems of the robot endeffector for generating the required impulsive forces, and demonstrate stick-juggling using real hardware.

To this end, we will use the framework developed in [3,4,29,30], where the complete control problem of the object and the robot is considered using a backstepping-like strategy.

Funding The authors acknowledge the support provided by the National Science Foundation, Grant CMMI-2043464.

Data availability The datasets generated during and/or analyzed during the current study are available from the corresponding author on reasonable request.

Declarations

Conflict of interest The authors declare that they do not have any conflict of interest.

Appendix: Steady precession of stick on hoop

For continuous motion of the stick, which was described in Sect. 7.2, we already have $\dot{\beta} = \dot{\beta}^* = 0$ and $\phi = \phi^* = 0$. To derive the remaining eight expressions in (61), we first write the expressions for the force on the stick and its point of application:

$$\mathbf{F} = F^* \begin{bmatrix} -\cos\alpha\cos\beta^* \\ -\sin\alpha\cos\beta^* \\ \sin\beta^* \end{bmatrix}, \quad \mathbf{r} = r^* \begin{bmatrix} \cos\alpha\sin\beta^* \\ \sin\alpha\sin\beta^* \\ \cos\beta^* \end{bmatrix}$$
(62)

where α indicates the angle of precession. The motion of the center-of-mass is described by the differential equation

$$\dot{\mathbf{h}} = \mathbf{v}, \qquad \dot{\mathbf{v}} = \frac{\mathbf{F}}{m} + \begin{bmatrix} 0 & 0 & -g \end{bmatrix}^{\mathrm{T}}$$
 (63)

with \mathbf{h} and \mathbf{v} defined in (3). The angular dynamics is governed by the relation

$$\dot{\mathbf{H}} = \mathbf{r} \times \mathbf{F} = F^* r^* \begin{bmatrix} \sin \alpha \\ -\cos \alpha \\ 0 \end{bmatrix}$$
 (64)

where **F** and **r** are given in (62). The last equation implies H_z is constant. Using (6) and (7), we get

$$H_z = J\dot{\alpha}\sin^2\beta^* = \text{constant} \quad \Rightarrow \quad \dot{\alpha} = \text{constant}$$
 (65)

By denoting the constant value of $\dot{\alpha}$ by $\dot{\alpha}^*$ and comparing \dot{H}_x and \dot{H}_y in (64) with the derivatives of H_x and H_y in (6), we get

$$J\dot{\alpha}^{*2}\sin\beta^*\cos\beta^* = F^*r^* \tag{66}$$



The motion of the center-of-mass in (63) can be expressed in the reference frame of the juggler by multiplying both sides of both equations by $\mathbf{R}_z^{\mathrm{T}}(\alpha)$; this yields

$$\dot{\bar{\mathbf{h}}} = \bar{\mathbf{v}}, \qquad \dot{\bar{\mathbf{v}}} = \frac{F^*}{m} \begin{bmatrix} -\cos\beta^* \\ 0 \\ \sin\beta^* \end{bmatrix} - \begin{bmatrix} 0 \\ 0 \\ g \end{bmatrix} \tag{67}$$

Since \bar{h}_z is constant, we have

$$\bar{v}_z = \bar{v}_z^* = 0 \quad \Rightarrow \quad \dot{\bar{v}}_z = 0 \tag{68}$$

Using $\dot{\bar{v}}_z = 0$, we get from (67)

$$F^* = mg/\sin\beta^* \tag{69}$$

We now make the choice

$$r^* = \ell/(2p^2), \qquad p \ge 1$$
 (70)

such that the point of application of the force satisfies $r=r^*, 0 \le r^* \le \ell/2$. Substituting (69) and (70) in (66), we obtain

$$\dot{\alpha}^* = \frac{1}{p} \sqrt{\frac{mg\ell}{2J\sin^2\beta^*\cos\beta^*}} \tag{71}$$

The center-of-mass of the stick undergoes uniform circular motion with a radius $\bar{h}_x = \bar{h}_x^*$; therefore, we have

$$\bar{v}_r^* = 0, \qquad \dot{\bar{v}}_r^* = -\dot{\alpha}^{*2} \bar{h}_r^*$$
(72)

Comparing the expressions for $\dot{\bar{v}}_x^*$ in (67) and (72) and substituting the value of $\dot{\alpha}^*$ in (71), we get

$$\bar{h}_x^* = \frac{2p^2 J \sin \beta^* \cos^2 \beta^*}{m\ell} \tag{73}$$

For the motion of the center-of-mass of the stick, we can also write

$$\bar{h}_{y}^{*} = 0, \quad \bar{v}_{y}^{*} = \dot{\alpha}^{*} \bar{h}_{x}^{*}$$
 (74)

Substituting (71) and (73) in the expression for \bar{v}_y^* , we get

$$\bar{v}_y^* = p \sqrt{\frac{2Jg\cos^3\beta^*}{m\ell}} \tag{75}$$

Equations (68)–(75) verify the expressions in (61).

References

- 1. Antsaklis, P.J., Michel, A.N.: A Linear Systems Primer. Birkhäuser, Boston (2007)
- Brogliato, B.: Nonsmooth Mechanics: Models, Dynamics and Control. Communications and Control Engineering. Springer, London (1999)

- Brogliato, B., Rio, A.Z.: On the control of complementaryslackness juggling mechanical systems. IEEE Trans. Autom. Control 45(2), 235–246 (2000)
- Brogliato, B.: Feedback control of multibody systems with joint clearance and dynamic backlash: a tutorial. Multibody Syst. Dyn. 42(3), 283–315 (2018)
- Brogliato, B., Mabrouk, M., Rio, A.Z.: On the controllability of linear juggling mechanical systems. Syst. Control Lett. 55(4), 350–367 (2006)
- Goebel, R., Sanfelice, R.G., Teel, A.R.: Hybrid Dynamical Systems: Modeling, Stability, and Robustness. Princeton University Press, Princeton (2012)
- Grizzle, J.W., Abba, G., Plestan, F.: Asymptotically stable walking for biped robots: analysis via systems with impulse effects. IEEE Trans. Autom. Control 46(1), 51–64 (2001)
- Kant, N., Mukherjee, R.: Orbital stabilization of underactuated systems using virtual holonomic constraints and impulse controlled poincaré maps. Syst. Control Lett. 146, 104813 (2020)
- Kant, N., Mukherjee, R.: Non-prehensile manipulation of a devil-stick: planar symmetric juggling using impulsive forces. Nonlinear Dyn. 103(3), 2409–2420 (2021)
- Kant, N., Mukherjee, R.: Juggling a devil-stick: hybrid orbit stabilization using the impulse controlled poincaré map. IEEE Control Syst. Lett. 6, 1304–1309 (2022)
- Kant, N., Mukherjee, R., Chowdhury, D., Khalil, H.K.: Estimation of the region of attraction of underactuated systems and its enlargement using impulsive inputs. IEEE Trans. Robot. 35(3), 618–632 (2019)
- Lynch, K.M., Mason, M.T.: Dynamic underactuated nonprehensile manipulation. In: Proceedings of IEEE/RSJ International Conference on Intelligent Robots and Systems, IROS '96, vol. 2, pp. 889–896 (1996)
- Lynch, K.M., Black, C.K.: Recurrence, controllability, and stabilization of juggling. IEEE Trans. Robot. Autom. 17(2), 113–124 (2001)
- Lynch, K.M., Mason, M.T.: Dynamic nonprehensile manipulation: controllability, planning, and experiments. Int. J. Robot. Res. 18(1), 64–92 (1999)
- Lynch, K.M., Murphey, T.D.: Control of nonprehensile manipulation. In: Control Problems in Robotics, pp. 39–57. Springer, Berlin (2003)
- Mason, M.T.: Progress in nonprehensile manipulation. Int. J. Robot. Res. 18(11), 1129–1141 (1999)
- Nakamura, K., Nakaura, S., Sampei, M.: Enduring rotary motion experiment of devil stick by general-purpose manipulator. In: Ulbrich, H., Ginzinger, L. (eds.) Motion and Vibration Control, pp. 241–251. Springer, Dordrecht (2009)
- Nakaura, S., Kawaida, Y., Matsumoto, T., Sampei, M.: Enduring rotary motion control of devil stick. IFAC Proc. 37, 805–810 (2004)
- Nersesov, S.G., Chellaboina, V., Haddad, W.M.: A generalization of Poincaré's theorem to hybrid and impulsive dynamical systems. In: Proceedings of the 2002 American Control Conference (IEEE Cat. No. CH37301), vol. 2, pp. 1240–1245. IEEE (2002)
- Reist, P., D'Andrea, R.: Design and analysis of a blind juggling robot. IEEE Trans. Robot. 28(6), 1228–1243 (2012)



- Ronsse, R., Lefevre, P., Sepulchre, R.: Rhythmic feedback control of a blind planar juggler. IEEE Trans. Robot. 23(4), 790–802 (2007)
- Ruggiero, F., Lippiello, V., Siciliano, B.: Nonprehensile dynamic manipulation: a survey. IEEE Robot. Autom. Lett. 3(3), 1711–1718 (2018)
- Sanfelice, R.G., Teel, A.R., Sepulchre, R.: A hybrid systems approach to trajectory tracking control for juggling systems. In: 46th IEEE Conference on Decision and Control, pp. 5282–5287 (2007)
- Schaal, S., Atkeson, C.G.: Open loop stable control strategies for robot juggling. In: Proceedings IEEE International Conference on Robotics and Automation, vol. 3, pp. 913– 918 (1993)
- Shiriaev, A., Robertsson, A., Freidovich, L., Johansson, R.: Generating stable propeller motions for devil stick. In: Proceedings of 3rd IFAC Workshop on Lagrangian and Hamiltonian Methods for Nonlinear Control (2006)
- Tornambe, A.: Modeling and control of impact in mechanical systems: theory and experimental results. IEEE Trans. Autom. Control 44(2), 294–309 (1999)
- Spong, M.W.: Impact controllability of an air hockey puck. Syst. Control Lett. 42(5), 333–345 (2001)

- Zachary Woodruff, J., Lynch, K.M.: Planning and control for dynamic, nonprehensile, and hybrid manipulation tasks. In: IEEE International Conference on Robotics and Automation (ICRA), pp. 4066–4073 (2017)
- Zavala-Rio, A., Brogliato, B.: On the control of a one degreeof-freedom juggling robot. Dyn. Control 9(1), 67–90 (1999)
- Zavala-Rio, A., Brogliato, B.: Direct adaptive control design for one-degree-of-freedom complementary-slackness jugglers. Automatica 37(7), 1117–1123 (2001)

Publisher's Note Springer Nature remains neutral with regard to jurisdictional claims in published maps and institutional affiliations.

Springer Nature or its licensor holds exclusive rights to this article under a publishing agreement with the author(s) or other rightsholder(s); author self-archiving of the accepted manuscript version of this article is solely governed by the terms of such publishing agreement and applicable law.

